Parametric Optimization of Structures Under Combined Base Motion Direct Forces and Static Loading

Izhak Bucher
Faculty of Mechanical Engineering,
Technion, Israel Institute of Technology,
Haifa 32000, Israel
e-mail: bucher@technion.ac.il

This paper deals with the optimization of vibrating structures as a mean for minimizing unwanted vibration. Presented in this work is a method for automatic determination of a set of preselected design parameters affecting the geometrical layout or shape of the structure. The parameters are selected to minimize the dynamic response to external forcing or base motion. The presented method adjusts the structural parameters by solving an optimization problem in which the constraints are dictated by engineering considerations. Several constraints are defined so that the static deflection, the stress levels and the total weight of the structure are kept within bounds. The dynamic loading acting upon the structure is described in this work by its power spectral density, with this representation the structure can be tailored to specific operating conditions. The uncertain nature of the excitation is overcome by combining all possible spectra into one PSD encompassing all possible loading patterns. An important feature of the presented method is its numerical efficiency. This feature is essential for any reasonably sized problem as such problems are usually described by thousands of degrees of freedom arising from a finite-element idealization of the structure. In this paper, efficient, closed form expressions, for the cost function and its gradients are derived. Those are computed with a partial set of eigenvectors and eigenvalues thus increasing the efficiency further. Several numerical examples are presented where both shape optimization and the selection of discrete components are illustrated. [DOI: 10.1115/1.1424888]

1 Introduction

The optimization of structures and machines with respect to their specific tasks has always been an important goal for designers and engineers. In particular, the optimization of flexible machine elements subject to dynamic loading patterns is usually carried out in order to minimize unwanted vibrations.

The design process of a structural element often begins by taking into account only static loading and self-weight; unfortunately this approach may lead to a design that performs badly under dynamic loading conditions. On the other hand, structures that are optimized with respect to dynamic loads are often lighter and smaller compared to their statically optimized counterparts. Despite the larger size and weight of statically optimized structures, they are often inferior in terms of their response to dynamic loads. Similarly structures that are designed with only direct forcing in mind may posses high vibration levels under base-motion which is often encountered in elements mounted on moving platforms and vehicles.

This work presents a formulation that takes all the abovementioned factors under consideration. Combined in the problem are the effects of: base-motion, static-loading and directly applied dynamic forces. It is thus expected that the proposed method will produce different result than what would have been achieved by considering separately only one of the loading types and would therefore give rise to more robust designs.

Minimization of vibration by modification of the geometry may require a huge computational effort, and this effort may even increase greatly when general loading conditions are considered. In this work, a special formulation that is aimed at reducing the computational effort considerably is presented.

Contributed by the Technical Committee on Vibration and Sound for publication in the JOURNAL OF VIBRATION AND ACOUSTICS. Manuscript received November 1997; Revised May 1998. Associate Editor: B. Yang.

Optimization as a mean for achieving a better structural design is a well-established area in the literature. Kirsh [1] and Haftka [2] have considered several structural optimization problems where mainly static loads or problems in which the maximization of one of the eigenvalues are presented via a quasi-static formulation of the response. In the past, several authors have applied analytical methods, Turner [3], Taylor [4] have used calculus of variations to determine (or to maximize) the first natural eigenvalues of a vibrating structure assuming that this would make the optimized design stiffer under dynamical loads. Realistic engineering structure requires numerical modeling and indeed, Kamat [5] analyzed a similar problem using finite element modeling, where he also was seeking to optimize the eigenvalues of a vibrating beam. Shape optimization using boundary elements is reported in Yamazaki [6] and in Brebbia [7], who chose to minimize the total weight subject to stress and displacement constraint.

Sinusoidal vibrations are often minimized by means of adding dynamic mass absorbers to a structure. These devices have low impedance close to a preselected frequency and reduce the vibration in the structure in the vicinity of a chosen frequency region. Ran and Elhay [8] presented a generalization for a multi-degree-of-freedom dynamic absorber where more than one frequency can be suppressed. Optimum design of dynamic absorbers for a system subjected to random (white noise) excitation is presented in Asami [9]. A review paper dealing with the optimization of structures subject to impact loading was recently published (Uwe and Pilkey [10]). In this work a direct nonlinear programming approach is described and some attention is devoted to nonlinear structures. Also in this work is the use of an adjoint variable based approach, but the associated heavy computational load, which is typical to such direct-approach methods, is inevitable.

In the past, due to lack of computing power and lack of modeling capabilities, only simple structures under a few idealized excitation patterns (i.e., sine, random, impulse) were optimized.

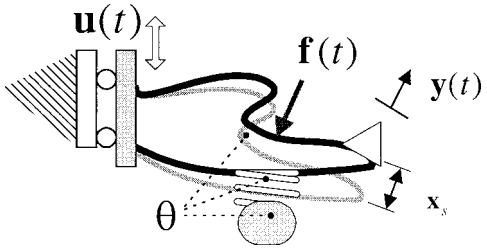

Fig. 1 Schematic representation of structure to be optimized

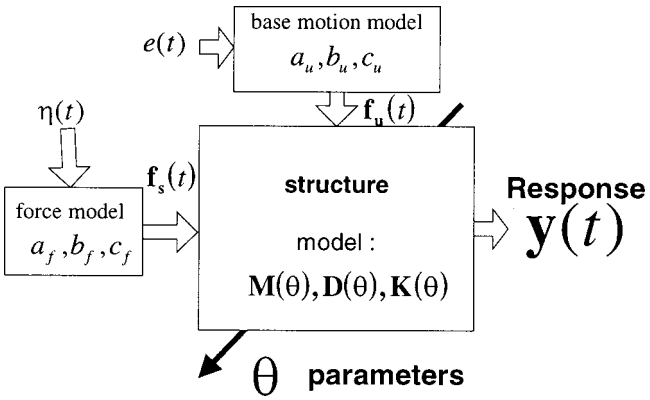

Fig. 2 Schematic representation of structure to be optimized

Over simplified models usually yield structures that are optimal for a narrow range of operation while a slight change in the frequency of excitation, could cause high vibration levels. The minimization of the vibratory level subject to realistic excitation patterns (mostly defined statistically by their power spectral density) may lead to a computationally intensive process solving a high-dimensional nonlinear optimization problem as described in this paper. A partial analytical solution and a numerical decomposition that is presented here, attempt to overcome these shortcomings.

The paper is organized as following: In the first section the problem at hand and its general formulation is described. The modeling of the structure and the excitation are presented in section 2 and the formulation leading to efficient evaluation of the objective function and its gradients follow in section 3. Section 4 presents some numerical issues concerning the choice of algorithm and parametrization of the geometry. In section 5 some numerical examples are shown and the conclusions are provided in section 6. Several appendices contain some details and are not essential for the main results but convey some information needed in the detailed formulation of the problem at hand.

1.1 Problem Definition. The problem dealt with in this paper is illustrated schematically in Fig. 1, which shows a structure whose geometry as well as some properties of discrete vibration absorbing devices are optimized. The structure is subject to base-motion, $\mathbf{u}(t)$ and to a directly applied force, $\mathbf{f}(t)$. The response at some reference points—$\mathbf{y}(t)$ is sought to be reduced. Also shown is the deformed structure due to static loading where the static deflection at the reference points is indicated by $\mathbf{x}_s$. This problem is mathematically defined below:

Optimization problem:

$$\underset{\theta}{minimize}\ J(\mathbf{y}) \tag{1}$$

subject to

a: weight limitation:	$mass(\theta) \leq \overline{M}$
b: static deflection	$\mathbf{x_s}(\theta) \leq \overline{\mathbf{x}}$
c: geometric constraints	$\mathbf{G} \leq \mathbf{g}(\theta) \leq \overline{\mathbf{G}}$
d: dynamics	$\mathbf{M}(\theta)\ddot{\mathbf{x}}(t)+\mathbf{D}(\theta)\dot{\mathbf{x}}(t)+\mathbf{K}(\theta)\mathbf{x}(t)=\mathbf{f}(t)$, $\mathbf{y}(t)=\mathbf{C}(\theta)\mathbf{x}(t)$
e: base motion	$\mathbf{x_u}(t)=\mathbf{u}(t), \quad PSD[\mathbf{u}(t)]=\mathbf{S}_{uu}(\omega)$
f: direct force	$\mathbf{f}(t), \quad PSD[\mathbf{f}(t)]=\mathbf{S}_{ff}(\omega)$

The optimization problem seeks an optimal vector of parameters, θ which minimizes a measure of the response $J(\mathbf{y})$ while not violating any of the constraints. In this work the cost function represents the RMS of the response under dynamic excitation. The constraints (**a-f**) are described in more detail below and in appendix D.

The main contributions of this paper are:

(a) The formulation of the problem is cast in a manner that enables one to approach this problem with a relative ease and to obtain a realizable design

(b) The incorporation of general loading types where uncertainty in their exact nature can be defined and handled automatically

(c) The introduction of a very efficient scheme for evaluating the cost function and the gradients using partial modal (eigenvalues and eigenvectors) data for this general type of loading

(d) The ability to realize the optimal geometry of a structure is ensured by providing a suitable construction of the geometry as a combination of smooth functions

The general formulation that is presented here is composed of many details where the constraints, the realization of the excitation and representation of the geometry all require careful attention. In this paper an attempt is being made to highlight some of the considerations that are believed to be central to such an optimization problem.

The model of the structure, which is depicted in Fig. 1, is optimized with respect to excitation patterns that are defined by means of their power spectral density (PSD). The excitation models are embedded in a global model as described in Fig. 2:

Where a_f, b_f, c_f and a_u, b_u, c_u define the power-spectral density of the external forces and the base motion, respectively (more detailed description is given in section 2.1).

In order to allow the usage of a standard and yet numerically efficient formulation, the overall model assumes white noise (or impulsive) inputs (Skelton [11]). The blocks appearing in Fig. 2 represent a shaping model for the force and the base motion as well as the optimized structure.

2 Modeling the Dynamic Response and the Combined Excitation

In order to optimize the parameters affecting the dynamic response of a structure, a model allowing one to predict the structural response under various conditions is developed. The model shown here in partitioned form follows the guidelines of Eq. (1):

$$\begin{bmatrix} \mathbf{M_{ss}} & \mathbf{M_{su}} & \mathbf{M_{sb}} \\ \mathbf{M_{us}} & \mathbf{M_{uu}} & M_{\mathbf{ub}} \\ \mathbf{M_{bs}} & \mathbf{M_{bu}} & \mathbf{M_{bb}} \end{bmatrix} \begin{pmatrix} \ddot{\mathbf{x}}_\mathbf{s} \\ \ddot{\mathbf{x}}_\mathbf{u} \\ \ddot{\mathbf{x}}_\mathbf{b} \end{pmatrix} + \begin{bmatrix} \mathbf{D_{ss}} & \mathbf{D_{su}} & \mathbf{D_{sb}} \\ \mathbf{D_{us}} & \mathbf{D_{uu}} & \mathbf{D_{ub}} \\ \mathbf{D_{bs}} & \mathbf{D_{bu}} & \mathbf{D_{bb}} \end{bmatrix} \begin{pmatrix} \dot{\mathbf{x}}_\mathbf{s} \\ \dot{\mathbf{x}}_\mathbf{u} \\ \dot{\mathbf{x}}_\mathbf{b} \end{pmatrix} + \begin{bmatrix} \mathbf{K_{ss}} & \mathbf{K_{su}} & \mathbf{K_{sb}} \\ \mathbf{K_{us}} & \mathbf{K_{uu}} & \mathbf{K_{ub}} \\ \mathbf{K_{bs}} & \mathbf{K_{bu}} & \mathbf{K_{bb}} \end{bmatrix} \begin{pmatrix} \mathbf{x}_\mathbf{s} \\ \mathbf{x}_\mathbf{u} \\ \mathbf{x}_\mathbf{b} \end{pmatrix} = \begin{pmatrix} \mathbf{f}_\mathbf{s} \\ \mathbf{f}_\mathbf{u} \\ \mathbf{0} \end{pmatrix} \tag{2}$$

Here: $\mathbf{x_s}$ indicates the unconstrained structural degrees of freedom

$\mathbf{x_u}$ structural degrees of freedom having prescribed motion, $\mathbf{x}_u = \mathbf{u}$

$\mathbf{x_b}$ structural degrees of freedom constrained to zero, $\mathbf{x}_b = \mathbf{0}$

$\mathbf{f_s}$ force acting at structural degrees of freedom

$\mathbf{f_u}$ reaction force caused by the base motion

Substituting the constraints, $\mathbf{x_u} = \mathbf{u}$ and $\mathbf{x_b} = \mathbf{0}$, into Eq. (2), we obtain:

$$\mathbf{M_{ss}}\ddot{\mathbf{x}}_\mathbf{s} + \mathbf{D_{ss}}\dot{\mathbf{x}}_\mathbf{s} + \mathbf{K_{ss}}\mathbf{x_s} = \mathbf{M_{su}}\ddot{\mathbf{u}} + \mathbf{D_{su}}\dot{\mathbf{u}} + \mathbf{K_{su}}\mathbf{u} + \mathbf{f_s(t)} \tag{3}$$

The dynamics of the structure under the combined loading is described by Eq. (3), where the right-hand side term forms the combined external excitation. One can notice that the base motion $\mathbf{x_u} = \mathbf{u}$ yields right-hand size terms which depend upon the optimized parameters—θ, i.e. $\mathbf{M_{ss}} = \mathbf{M_{ss}}(\theta), .. \mathbf{K_{su}} = \mathbf{K_{su}}(\theta)$. The dependency upon θ is omitted from all the following equations for brevity.

The models of the displacement (base) excitations and the direct force $\mathbf{u}, \mathbf{f_s(t)}$ are developed and explained below.

2.1 Modeling the External Excitation. In order to perform the optimization under realistic excitation conditions one wishes to describe the variation of the applied force as a function of frequency as this information is often available from tests and standards. For that purpose, a shaping system is devised so that a fictitious white noise input to the model (i.e., a force having equal magnitude for all frequencies) is mathematically modified so that the true nature of the excitation is captured. The shaped force is internal to the global model with a predefined power spectral density (PSD).

A linear shaping system is defined below by $\mathbf{a_u}$, $\mathbf{b_u}$, $\mathbf{c_u}$ where the output $\mathbf{u(t)}$ representing the base motion has the required properties.

$$\begin{aligned} \dot{\mathbf{q}}_\mathbf{u}(t) &= \mathbf{a_u}\mathbf{q_u}(t) + \mathbf{b_u}\mathbf{e}(t) \\ \mathbf{u}(t) &= \mathbf{c_u}\mathbf{q_u}(t) \end{aligned} \tag{4}$$

Here $\mathbf{q}_u(t)$ is the internal state vector. In order to assure that $\mathbf{u}(t)$ and its first time-derivative are finite, the model must comply with the following constraint:

$$\mathbf{c_u}\mathbf{b_u} = \mathbf{0}, \quad \mathbf{c_u}\mathbf{a_u}\mathbf{b_u} = 0 \tag{5}$$

Proof: See Appendix A. Using Eqs. (3,4,5) and Eqs. (A1,A2) we can express the reaction force due to the base motion as:

$$\mathbf{f_u} = \mathbf{M_{su}}\ddot{\mathbf{u}} + \mathbf{D_{su}}\dot{\mathbf{u}} + \mathbf{K_{su}}\mathbf{u} = [\mathbf{K_{su}} \quad \mathbf{D_{su}} \quad \mathbf{M_{su}}] \begin{bmatrix} \mathbf{c_n} \\ \mathbf{c_u}\mathbf{a_u} \\ \mathbf{c_u}\mathbf{a_u^2} \end{bmatrix} \mathbf{q_u} \tag{6}$$

Assuming proportional damping i.e., $\mathbf{D} = \alpha\mathbf{M} + \beta\mathbf{K}$, Eq. (6) can becomes:

$$\mathbf{f_u} = (\mathbf{K_{su}}\mathbf{c_u} + (\alpha\mathbf{M_{su}} + \beta\mathbf{K_{su}})\mathbf{c_u}\mathbf{a_u} + \mathbf{M_{su}}\mathbf{c_u}\mathbf{a_u^2})\mathbf{q_u} \triangleq \mathbf{C_u}\mathbf{q_u} \tag{7}$$

One can note that $\mathbf{C}_u$ is a function of some structural parameters that depend upon the optimized parameter-vector θ.

In a completely analogous manner the directly applied force is described by a linear shaping system which is defined by:

$$\begin{aligned} \dot{\mathbf{q}}_f(t) &= \mathbf{a}_{ff}\mathbf{q}_f(t) + \mathbf{b}_f\eta(t) \\ \mathbf{f_s}(t) &= \mathbf{C}_f\mathbf{q}_f(t) \end{aligned} \tag{8}$$

The complete model is obtained by combining Eq. (3) with Eq. (4) and Eq. (8) in a state-space formulation as shown in the following section.

2.2 State-Space Realization of the Structure and the Excitation. It proves numerically convenient to convert the representation of the complete structure and the excitation into a state-space form. Using Eq. (3) we are able to write:

$$\dot{\mathbf{q}}_\mathbf{s} = \begin{bmatrix} \mathbf{0} & \mathbf{I} \\ -\mathbf{M_{ss}^{-1}}\mathbf{K_{ss}} & -\mathbf{M_{ss}^{-1}}\mathbf{D_{ss}} \end{bmatrix} \mathbf{q_s} + \begin{bmatrix} \mathbf{0} \\ \mathbf{M_{ss}^{-1}} \end{bmatrix} \Big(\mathbf{f_u}(t) + \mathbf{f_s}(t) \Big) \tag{9}$$

where $\mathbf{q_s} = \begin{pmatrix} \mathbf{x_s} \\ \dot{\mathbf{x}}_\mathbf{s} \end{pmatrix}$.

Combining Eqs. (4,8) with Eq. (9), the complete realization is formed:

$$\dot{\mathbf{q}} = \begin{bmatrix} \begin{bmatrix} \mathbf{0} & \mathbf{I} \\ -\mathbf{M_{ss}^{-1}}\mathbf{K_{ss}} & -\mathbf{M_{ss}^{-1}}\mathbf{D_{ss}} \end{bmatrix} & \begin{matrix} \mathbf{0} & \mathbf{0} \\ \mathbf{M_{ss}^{-1}}\mathbf{C_u} & \mathbf{M_{ss}^{-1}}\mathbf{C}_f \end{matrix} \\ \begin{matrix} \mathbf{0} \\ \mathbf{0} \end{matrix} & \begin{matrix} \mathbf{a_{uu}} & \mathbf{0} \\ \mathbf{0} & \mathbf{a_{ff}} \end{matrix} \end{bmatrix} \times \begin{pmatrix} \begin{pmatrix} \mathbf{x_s} \\ \dot{\mathbf{x}}_\mathbf{s} \end{pmatrix} \\ \mathbf{q_u} \\ \mathbf{q}_f \end{pmatrix} + \begin{pmatrix} \begin{pmatrix} \mathbf{0} \\ \mathbf{0} \end{pmatrix} \\ \mathbf{b_u} \\ \mathbf{b}_f \end{pmatrix} \begin{pmatrix} \mathbf{e}(t) \\ \eta(t) \end{pmatrix} \tag{10}$$

where $\mathbf{x}_s$, $\mathbf{q}_u$, $\mathbf{q}_g$ represent the structural, base motion and force related state vectors. And $\mathbf{e}(t)$, $\eta(t)$ are white noise processes.

The chosen response to be minimized is a linear combination of the state-variables in Eq. (10) where a natural choice (one of many) represents the response at point k relative to the base, in this case:

$$\mathbf{y}(t) = \mathbf{e}_k^T\mathbf{x}_s(t) - \mathbf{u}(t) = ((\mathbf{e}_k \quad \mathbf{0}) \quad -\mathbf{c_{uu}} \quad \mathbf{0})\mathbf{q}(t) \triangleq \mathbf{c_y}\mathbf{q}(t) \tag{11}$$

where $e_k = (0 \ldots 1 \ldots 0)$ (one at the kth location).

The output selected in Eq. (11) defines the requirement that the structure will follow the motion of the base despite its dynamic characteristics and despite the additional external loading.

3 Efficient Evaluation of the Cost Function and Its Gradients

During the optimization process the measure of the response, the cost function, needs to be evaluated many times. In addition to that, the gradient of this cost function needs to be computed, at every iteration, so that a direction of progression in the parameter space could be determined (see Fletcher [12]). Practical vibrating structures need to be represented by hundreds or thousands of degrees of freedom in order to form valid models. As an optimization process requires many evaluations of the cost function, any practical optimization scheme must compute the cost function and its derivatives efficiently in a reasonable amount of time. With this goal in mind the computational process, which is described in this section, was developed.

The cost function in this work $J(\mathbf{y})$ is defined in an analogous manner to Bucher and Braun [13]. Assuming random excitation (even though the mathematical development here is suitable for deterministic and transient cases, see Skelton [11]; Bucher and Braun [13]) we may write:

$$J(\mathbf{y}) = trE[\mathbf{y^T}(t)\mathbf{Q}\mathbf{y}(t)] \tag{12}$$

where $\mathbf{Q}$ is some weighting matrix $E[\cdot]$ indicates statistical expectation and $tr[\cdot]$ is the trace operator.

Equation (12) is in effect an expression for the weighted root mean square (RMS) of the output and for a linear time invariant system such as described by Eqs. (10, 11) it can expressed in terms of the state-covariance matrix, as the following:

$$J(\mathbf{y}) = trE[\mathbf{y^T}(t)\mathbf{Q}\mathbf{y}(t)] = tr[\mathbf{Q}\mathbf{c_y}\mathbf{R_{qq}}\mathbf{c_y^T}] \tag{13}$$

Where the state covariance, $\mathbf{R_{qq}}$ is the solution for the following Lyapunov equation: Skelton (1989); Junkins (1993).

$$\mathbf{A}\mathbf{R_{qq}} + \mathbf{R_{qq}}\mathbf{A^T} + \mathbf{B}\mathbf{R_{ff}}\mathbf{B^T} = \mathbf{0} \tag{14}$$

Here the $\mathbf{A}$, $\mathbf{B}$ matrices are the system and input matrices from Eq. (10).

Assuming that $\mathbf{e}(t)$, $\eta(t)$ are uncorrelated white noise processes, we have:

$$\mathbf{R_{ff}}=\begin{bmatrix}\mathbf{R_{ee}} & 0\\ 0 & \mathbf{R}_{\eta\eta}\end{bmatrix} \tag{15}$$

Every time one wishes to compute the cost function, Eq. (13), the Lyapunov equation (Eq. (14)) has to be solved. Although this equation has a high dimension, it can still be solved efficiently, as presented below.

Decomposing the total state-covariance matrix of Eq. (10), we may write:

$$\mathbf{R_{qq}}=\begin{bmatrix}\mathbf{R_{ss}} & \mathbf{R_{su}} & \mathbf{R_{sf}}\\ \mathbf{R_{us}} & \mathbf{R_{uu}} & \mathbf{R_{uf}}\\ \mathbf{R_{fs}} & \mathbf{R_{fu}} & \mathbf{R_{ff}}\end{bmatrix} \tag{16}$$

Substituting Eq. (16) in Eq. (14) and using Eqs. (10,15) we obtain 9 matrix equations of which 3 are redundant (due to symmetry of $\mathbf{R}_{qq}$) and can therefore be omitted. These reduced order equations can be solved in a particular order as described below.

3.1 State Covariance Equations. The partitioning of the state [Eq. (10)] allows us to solve some of the equations in a particular order and thus achieve significant saving in the computational effort. The first two equations to be solved define the dynamics of the base-motion and the direct force excitations

$$\mathbf{a_{uu}R_{uu}}+\mathbf{R_{uu}a_{uu}^T}+\mathbf{b_u R_{ee} b_u^T}=\mathbf{0} \tag{17}$$

$$\mathbf{a}_{ff}\mathbf{R_{ff}}+\mathbf{R_{ff}a}_{ff}^{\mathbf{T}}+\mathbf{b}_f\mathbf{R_{ee}b}_f^{\mathbf{T}}=\mathbf{0} \tag{18}$$

A single equation determines the (lack of) coupling between $\mathbf{f_s}$ and $\mathbf{f_u}$

$$\mathbf{a_{uu}R_{uf}}+\mathbf{R}_{\mathbf{fu}}^{\mathbf{T}}\mathbf{a}_{ff}^{\mathbf{T}}=\mathbf{0} \tag{19}$$

where the assumption that $\mathbf{e}(t)$, $\eta(t)$ are uncorrelated results in $\mathbf{R_{uf}}=\mathbf{0}$.

Two equations determine the effect of base motion and the effect of a directly applied force on the structural states $\mathbf{q_s}$. This effect is manifested via the cross covariance matrices $\mathbf{R_{sf}}$ and $\mathbf{R_{su}}$:

$$\mathbf{A_{ss}R_{sf}}+\mathbf{R}_{\mathbf{fs}}^{\mathbf{T}}\mathbf{a}_{ff}^{\mathbf{T}}+(\mathbf{B_{su}R_{uf}}+\mathbf{B_{sf}R_{ff}})=\mathbf{0} \tag{20}$$

$$\mathbf{A_{ss}R_{su}}+\mathbf{R}_{\mathbf{us}}^{\mathbf{T}}\mathbf{a}_{\mathbf{uu}}^{\mathbf{T}}+(\mathbf{B_{su}R_{uu}}+\mathbf{B_{sf}R_{fu}})=\mathbf{0} \tag{21}$$

The final equation to be solved in this sequence determines the sought structural state covariance:

$$\mathbf{A_{ss}R_{ss}}+\mathbf{R_{ss}A}_{\mathbf{ss}}^{\mathbf{T}}+(\mathbf{B_{su}R_{us}}+\mathbf{B_{sf}R_{fs}}+\mathbf{R}_{\mathbf{fs}}^{\mathbf{T}}\mathbf{B}_{\mathbf{sf}}^{\mathbf{T}}+\mathbf{R}_{\mathbf{us}}^{\mathbf{T}}\mathbf{B}_{\mathbf{su}}^{\mathbf{T}})=\mathbf{0} \tag{22}$$

The division of Eq. (14) into several equations, each having a lower size, allows us to write explicit expressions for the gradients. These equations form several Lyapunov equations as shown below.

3.2 Gradients of the Cost Function. The derivative of the cost function (the gradient) with respect to a single parameter, can be written as:

$$\frac{\partial \mathbf{J(y)}}{\partial\theta_k}=tr\left[\mathbf{Qc}_y\frac{\partial \mathbf{R}_{qq}}{\partial\theta_k}\mathbf{c}_\mathbf{y}^\mathbf{T}\right] \tag{23}$$

Equation (23) can be derived by differentiation of Eqs. (20, 21, 22) with respect to θ_k. Performing the required operations we arrive at a set of coupled Lyapunov equations that can be solved in a particular order so that once more, computational efficiency is gained.

Performing the differentiation we arrive at:

$$\mathbf{A_{ss}}\frac{\partial \mathbf{R_{sf}}}{\partial\theta_k}+\frac{\partial \mathbf{R}_{\mathbf{sf}}^{\mathbf{T}}}{\partial\theta_k}\mathbf{a}_{ff}^{\mathbf{T}}+\left(\frac{\partial \mathbf{A_{ss}}}{\partial\theta_k}\mathbf{R_{sf}}+\frac{\partial \mathbf{B_{sf}}}{g!\,\theta_k}\mathbf{R_{ff}}\right)=\mathbf{0} \tag{24}$$

$$\mathbf{A_{ss}}\frac{\partial \mathbf{R_{su}}}{\partial\theta_k}+\frac{\partial \mathbf{R}_{\mathbf{su}}^{\mathbf{T}}}{\partial\theta_k}\mathbf{a}_{\mathbf{uu}}^{\mathbf{T}}+\left(\frac{\partial \mathbf{A_{ss}}}{\partial\theta_k}\mathbf{R_{su}}+\frac{\partial \mathbf{B_{su}}}{\partial\theta_k}\mathbf{R_{uu}}\right)=\mathbf{0} \tag{25}$$

Having solved Eqs. (24, 25) we are able to extract $\partial \mathbf{R}_{ss}/\partial\theta_k$ from:

$$\mathbf{A_{ss}}\frac{\partial \mathbf{R_{ss}}}{\partial\theta_k}+\frac{\partial \mathbf{R_{ss}}}{\partial\theta_k}\mathbf{A}_{\mathbf{ss}}^{\mathbf{T}}+(\mathbf{W}+\mathbf{W}^{\mathbf{T}})=\mathbf{0} \tag{26}$$

where

$$\mathbf{W}\triangleq\frac{\partial \mathbf{A_{ss}}}{\partial\theta_k}\mathbf{R_{ss}}+\frac{\partial \mathbf{B_{su}}}{\partial\theta_k}\mathbf{R_{us}}+\mathbf{B_{su}}\frac{\partial \mathbf{R_{us}}}{\partial\theta_k}+\frac{\partial \mathbf{B_{sf}}}{\partial\theta_k}\mathbf{R_{fs}}+\mathbf{B_{sf}}\frac{\partial \mathbf{R_{fs}}}{\partial\theta_k}$$

Equation (23) needs to be computed for all the optimized parameters, i.e. for $k=1\ldots n_\theta$.

3.3 Solving the Coupled Covariance and Gradient Equations Efficiently. The computational effort which is required for solving Eq. (14) is proportional to n_q^3, where $\mathbf{R}_{qq}\in\Re^{n_q x n_q}$, additional effort is due to the gradient equations which require a computational effort proportional to $n_\theta n_q^3$ (where $\theta\in\Re^{n_0 x 1}$). Noticing the fact that all the equations e.g. Eqs. (17–26) have $\mathbf{A_{ss}}$, $\mathbf{a_{uu}}$ and $\mathbf{a}_{ff}$ as coefficients we can pre-invert or predecompose (see appendix C) these matrices only once per iteration and solve for the cost and the gradient equations at an effort proportional to n_s^3 where n_s is the number of degrees of freedom. The ability to solve $n_s<1/2n_q$ equations *once* rather than n_0+1 times reduces the computational effort by more than an order of magnitude. Still a significant saving in time is achieved by using a partial eigen-decomposition method (Parlett [14]) as shown in Bucher and Braun 1993. A complete eigen-decomposition of $\mathbf{A_{ss}}$ (and $\mathbf{A}_{\mathbf{ss}}^{\mathbf{T}}$) can be obtained from the eigen-decomposition of the mass and stiffness $\mathbf{M_{ss}}$, $\mathbf{K_{ss}}$ as is shown in Blucher and Braun 1993 and in a short form in Appendix C.

Some of the eigenvectors and eigenvalues of $\mathbf{M_{ss}}$, $\mathbf{K_{ss}}$ are obtained by an iterative solver (e.g. Lanczos, Parlett [14]) while the result from a previous iteration serves as an excellent initial guess for the next one. This fact adds more efficiency to the convergence of the solution.

4 Numerical Aspects of the Optimization Problem

In this section some measures for circumventing problems associated with the large optimization problem at hand are described.

4.1 Selection of the Optimization Algorithm. The size of the problem and the sub-problems being solved during the optimization process, may cause numerical deficiencies due to differences in scales and due to the discontinuity of the constraint boundaries. In this work, emphasis is being put upon the formulation of the physical problem and on efficiency of the cost function and gradients. The optimizer, which was used in this work, was taken from the Matlab™ optimization Toolbox and is hence completely documented elsewhere. The algorithm implemented there is a derivative of the sequential quadratic optimization approach (Fletcher [12]). Further investigations will concentrate on the optimization algorithm itself.

4.2 Using a Smooth Curve Representation for the Geometry. The optimization process does not generally guarantee that the obtained optimal set of parameters will give rise to a practically realizable structure. In order to improve the ability to manufacture the optimized structure, the geometry is parametrized by a curve (or surface) represented as a linear combination of n_θ smooth basis functions

$$p(\xi)=\sum_{i=1}^{n_0}\theta_i g_i(\xi) \tag{27}$$

where ξ is a coordinate along the geometry, $p(\xi)$ is the obtained curve (or surface), $g_i(\xi)$ are the basis functions and θ_i are parameters to be determined by the optimization process.

In reality the equations of motion may depend upon a set of piecewise constant parameters h_k, thus the projection of the h_k-dependent geometry onto the subspace of θ_i-dependent geometry provides the desired smoothed geometry.

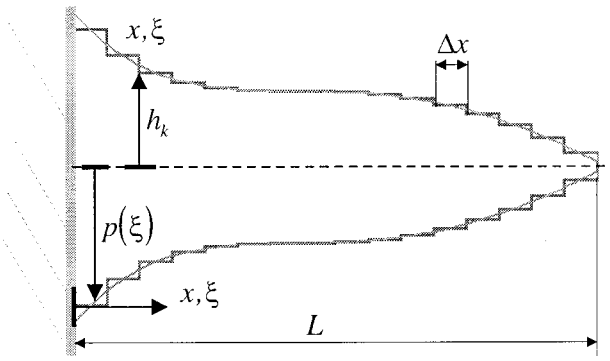

Fig. 3 Parametrization of the geometric representation of the structure to be optimized

The implications of this parametrization can be further clarified by an example, which is shown later in section 5. In this example the thickness of a beam is to be optimized as depicted in Fig. 3. The smooth curve $p(\xi)$ serves as a guideline for the actual parameters-h_k in a manner described below.

4.2.1 Projection of the Optimized Parameters and Computation of the Gradients. Let the geometry of the optimized structure be piecewise constant, i.e.:

$$h_k = p\left(k\frac{\Delta x}{L}\right) = \sum_{i=1}^{n_\theta} \theta_i g_i\left(k\frac{\Delta x}{L}\right), \quad k = 1 \ldots m \tag{28}$$

The coefficients θ_i are found from the geometrical parameters h_k by collecting Eq. (28) for all possible values. As a result a matrix equation is formed:

$$\begin{bmatrix} g_1(\xi_1) & g_2(\xi_1) & \cdots & \\ g_1(\xi_2) & g_2(\xi_2) & & \\ g_1(\xi_3) & g_2(\xi_3) & & \\ \vdots & \vdots & \vdots & g_n(\xi_m) \end{bmatrix} \begin{pmatrix} \theta_1 \\ \theta_2 \\ \vdots \\ \theta_{n_\theta} \end{pmatrix} = \begin{pmatrix} h_1 \\ h_2 \\ \vdots \\ h_m \end{pmatrix} \tag{29}$$

where the shorter notation $\mathbf{G}\theta = \mathbf{h}$ will be used.

While the optimization is being performed by varying θ, we use Eq. (29) to compute the actual geometric parameters h_k.
Since an expressions of the gradient $\partial J(\mathbf{y})/\partial\theta_k$ is also needed, we differentiate Eq. (29) to obtain:

$$\frac{\partial J(\mathbf{y})}{\partial \theta_i} = \sum_{k=1}^{m} \frac{\partial J}{\partial h_k}\frac{\partial h_k}{\partial \theta_i} \tag{30}$$

where a more compact matrix form yields, $(\partial J/\partial\theta) = \mathbf{G}^{\mathbf{T}}(\partial J/\partial \mathbf{h})$.

During the optimization we compute the gradient using the natural parameters of the problem (as described in section 3.2) and then we use Eq. (30) to obtain the projected gradient in terms of θ. The basis functions $g_i(\xi)$ were chosen so that $\mathbf{G}$ posses orthogonal columns thus, this transformation does not deteriorate the numerical conditioning of the problem.

4.3 Numerical Performance Benchmark. The performance of the optimization procedure depends mostly on the computing time of the cost function (computing the RMS of the response) and on the computing time of the gradients. The proposed method was compared with the most economical computation procedure known to the author (apart from the proposed algorithm) in the form of a frequency domain algorithm. This method uses a partial modal model of the structure where 6 modes were taken for the intermediate calculations. Both methods were timed for different model-sizes where the number of degrees of freedom of the model in Fig. 5 was varied. The results are depicted in Fig. 4.

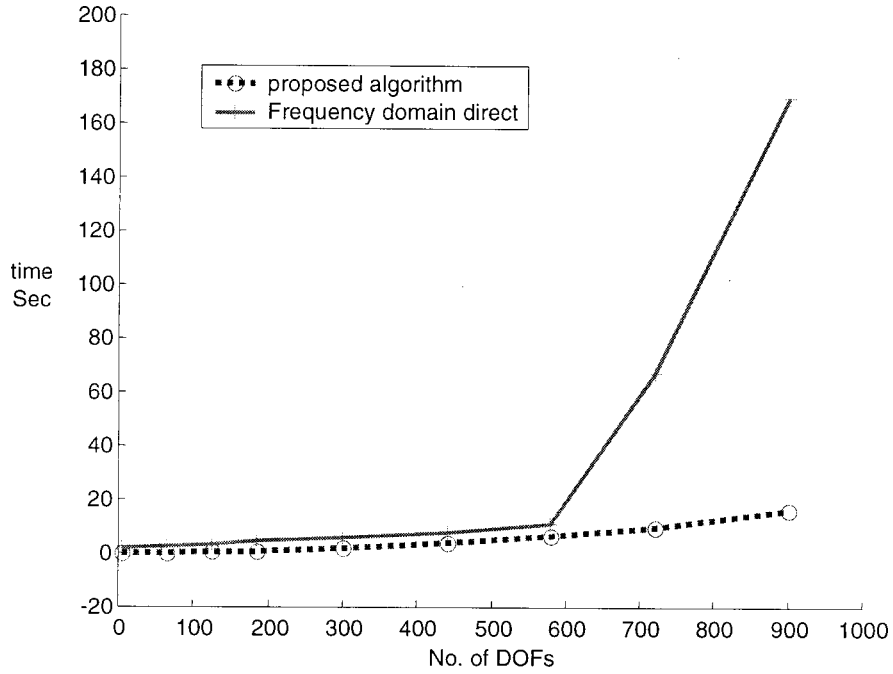

Fig. 4 Speed of execution of cost function, proposed method vs. frequency domain approach

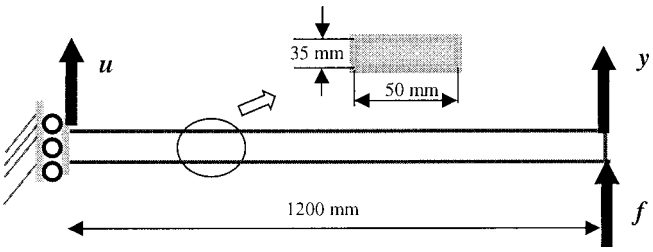

Fig. 5 Force and base motion of the initial structure

It can be observed in Fig. 4 that the proposed method executes faster than the frequency domain counterpart and the difference in speed becomes more significant as the size of the model increases. This increase is partly because of the smaller number of operations, but mainly due to the smaller storage space needed for the proposed algorithm. (The code was run on a Pentium III, 500 MHz with 128MB RAM.) It should be mentioned that the proposed method produces an analytical solution and is therefore exact while the frequency domain method performs and approximates calculation $RMS^2 = \sum_{\omega} |H(\omega)|^2 S_{uu}(\omega) \Delta\omega$, to approximate frequency domain integration. This approximation was found to slow down the convergence of the frequency domain method much beyond the ratio presented in Fig. 4. With the proposed method, the computation of the gradients produces a computational load, which is similar to the load of the cost function. The frequency domain method, on the other hand, would at best present a computation time, which is n_θ times longer than the computation of the cost function (n_θ being the number of optimized parameters, each needs to be perturbed in a finite difference scheme).

5 Illustrative Examples and Test-Cases

In this section several test cases are presented. In the first case the geometry (profile) of a Bernouli-Euler beam is optimized under several loading conditions. The result of the optimization process is compared for several combinations of loading patterns and conclusions are being made. In the second example an array of spring-mass systems spread along a beam is optimized with respect to a specific loading pattern.

5.1 Case A-Optimizing a Beam's Profile. In this example, the vibratory response as defined in Eq. (1) is sought to be minimized. The parameters of the optimization are illustrated in Fig. 3 and the loading pattern is composed of a direct force $-f$ in addition to motion of the base u as (shown in Fig. 5)

The optimization is carried out for the following cases:
case (A-I) Direct force excitation $-f$
case (A-II) Base motion excitation $-u$
case (A-III) Combined base motion and direct force $-u$ and f
case (A-IV) Combined base motion and direct force $-u$ and f − no static constraint (constraint b in equation 1 is removed)

In all the above cases the material properties were $E = 70$GPa, $\rho = 2600$ kg/m^3 The results of each case are depicted in Figs. 6, 7:

5.1.1 Discussion for Examples A-I,II,III,IV. In this example the response at the tip was minimized under various excitations and constraints. The total mass of the structure was not allowed to increase more than 40 percent of the original one. The structure was divided into 44 elements, but only the first 6 modes were considered. A band-pass filter 20 to 20.3 Hz modeled the PSD of the excitations (both for force and base motion).

Examples A-I and A-II show that an identical PSD assigned to the force and base motion excitations, yields different optimized shapes (See Figs. 6a,c). This illustrates the importance of considering the right type of excitation—base motion or direct force. A combined excitation in example A-II (Figs. 6e,f) gives rise to a shape and response reduction, which seem to lie between cases A-I and A-II. The largest reduction in the response was achieved for case A-IV (see Table 1, reduction of 1001 of the initial RMS). Despite this large reduction, the structure became very soft for static loads to a degree that it is no longer practical (noticeable in Fig. 7f). The last example emphasizes the importance of the engineering constraints.

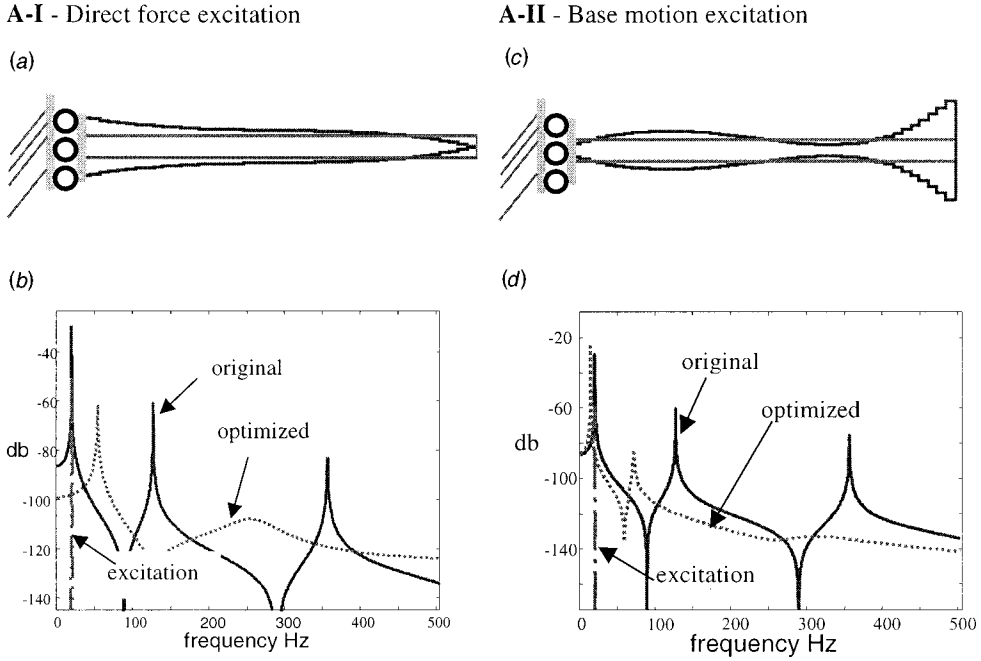

Fig. 6 Case A-I: (*a*) shape of original and optimized beam under direct force (*b*) frequency response and excitation PSD; Case A-II: (*c*) shape of original and optimized beam under base motion (*d*) frequency response and excitation PSD

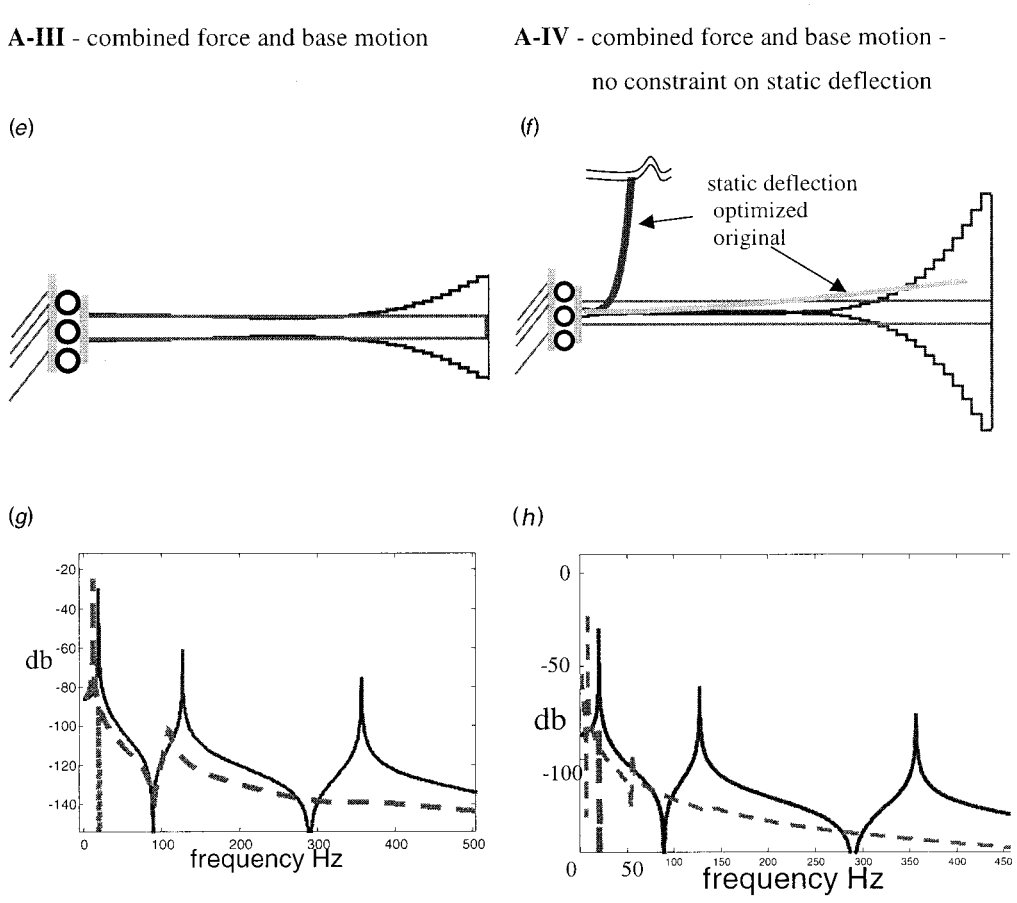

Fig. 7 Case A-III: (*e*) shape of original and optimized beam under combined direct force and base motion (*f*) frequency response and excitation PSD; case A-IV (*g*) shape of original and optimized beam under combined direct force and base motion—no constraint on static deflection (*h*) frequency response and excitation PSD

5.2 Case B-Optimizing an Array of Dynamic Mass Absorbers Connected to a Beam. In the second example, 11 dynamic mass absorbers are being tuned in order to minimize the effect of a nonsinusoidal force acting at the tip at the structure. A schematic description of the system is provided in Fig. 8.

The optimization has constraints on the values of the springs, the mass and the total amount of added mass to assure positive values for mass and stiffness of the added devices.

The results for a specific geometry and direct force loading are depicted below.

5.2.1 Discussion for Case B. The problem of tuning an array of dynamic mass absorbers was treated using the proposed optimization method. The method automatically tunes the spring-rates and mass values so that the response is minimized with respect to the power spectral distribution of force as shown in Fig. 9. As a result, the natural frequencies of the optimized array of dynamic mass absorbers was distributed in the frequency range where the force has significant influence. This result is neither anticipated nor described in the literature. The total RMS was reduced by an order of magnitude and a reduction in the response is evident for a range of frequencies (see Fig. 9) and thus the usefulness of the proposed method is evident.

6 Conclusions

In this paper a computationally efficient strategy for parametric optimization of structures was presented. The method takes into consideration realistic external loading types that can be defined by means of their power spectral density. The formulation of the problem incorporates several constraints that assure meaningful results in the engineering sense and an example demonstrates the effect of not including such an overall approach. A closed form solution for the cost function and its gradients was presented; thus both accuracy and computational speed are gained during the optimization process. The effectiveness of the proposed method was successfully demonstrated via several numerical case studies. New results are shown for tuning an array of dynamic mass ab-

Table 1 Reduction factor in the RMS response for cases A-I.II,II,IV

A-I direct force	A-II base motion	A-III Combined, force and base motion	A-IV Combined, no static deflection constraint
380.78	66.96	105.1	1001

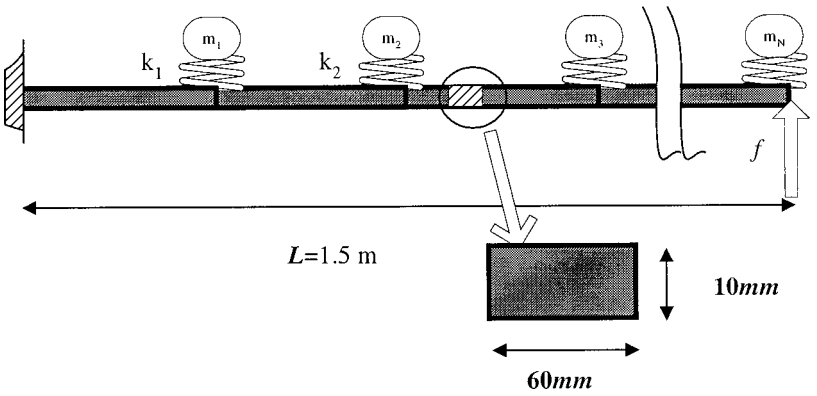

Fig. 8 An array of dynamic mass-absorbers

sorbers under broad band excitation. The proposed method paves the way towards practical optimization of engineering structures that are represented by finite element models.

Appendix A—Conditions for Physical Realizability of the Excitation Model

Given the power spectral density of the base-motion we need to realize a fictitious filter as shown in Eq. (8). This realization is subject to some physical constraints assuring that the output of such filter will be finite for the first and the second derivatives with respect to time, i.e..:

$$\dot{\mathbf{u}}(\mathbf{t}) = \mathbf{c_f}\dot{\mathbf{q}}_\mathbf{u}(t) = \mathbf{c_f a_f q_u}(t) + \mathbf{c_f b_f e}(t) \tag{A1}$$

and

$$\ddot{\mathbf{u}}(t) = \mathbf{c_f}\ddot{\mathbf{q}}_\mathbf{u}(t) = \mathbf{c_f a_f a_f q_u}(t) + \mathbf{c_f a_f b_f e}(t) + \mathbf{c_f b_f}\dot{\mathbf{e}}(t) \tag{A2}$$

In order to assure that the applied force due to base motion possesses a finite energy contents, we would need to have both $\ddot{\mathbf{u}}(t)$, $\dot{\mathbf{u}}(t)$ square integrable. As $\mathbf{e}(t)$ being white noise, $\int_0^\infty |\mathbf{e}(t)|^2 dt$ is by no means finite, therefore putting

$$\mathbf{c_f b_f} = 0, \quad \mathbf{c_f a_f b_f} = 0 \tag{A3}$$

in Eqs. (*A*1,*A*2) this difficulty is removed.

The displacement shaping filter can be expressed in a transfer function form between the input $e(t)$-(white noise) and the output $u(t)$:

Using the Markov parameters (Skelton, 1989), we have for the displacement

$$H(s) = \frac{u(s)}{e(s)} = \sum_{i=1}^{\infty} \frac{c_f a_f^i b_f}{s^i} = \frac{c_f b_f}{s} + \frac{c_f a_f b_f}{s^2} + \cdots \tag{A4}$$

and for the acceleration we obtain

$$\tilde{H}(s) = \frac{\ddot{u}(s)}{e(s)} = s^2 \sum_{i=1}^{\infty} \frac{c_f a_f^i b_f}{s^i} = s c_f b_f + c_f a_f b_f + \frac{c_f a_f^2 b_f}{s} + \cdots \tag{A5}$$

For physical reasons we wish to have $\lim_{\omega \to \infty} \tilde{H}(j\omega) = 0$. (This is to assure finite response at high frequencies), therefore Eq. (13) needs to be fulfilled.

A filter having this property will have a pole excess of three over the number of zeros.

Appendix B—Definitions of Main Matrices

Several matrices being used in this paper are defined here:

$$\mathbf{A} = \begin{bmatrix} \begin{bmatrix} \mathbf{0} & \mathbf{I} \\ -\mathbf{M}_{ss}^{-1}\mathbf{K}_{ss} & -\mathbf{M}_{ss}^{-1}\mathbf{D}_{ss} \end{bmatrix} & \begin{matrix} \mathbf{0} \\ \mathbf{M}_{ss}^{-1}\mathbf{C}_u \end{matrix} & \begin{matrix} \mathbf{0} \\ \mathbf{M}_{ss}^{-1}\mathbf{C}_f \end{matrix} \\ \begin{matrix} \mathbf{0} & \mathbf{0} \end{matrix} & \begin{matrix} \mathbf{a_{uu}} \\ \mathbf{0} \end{matrix} & \begin{matrix} \mathbf{0} \\ \mathbf{a_{gg}} \end{matrix} \end{bmatrix},$$

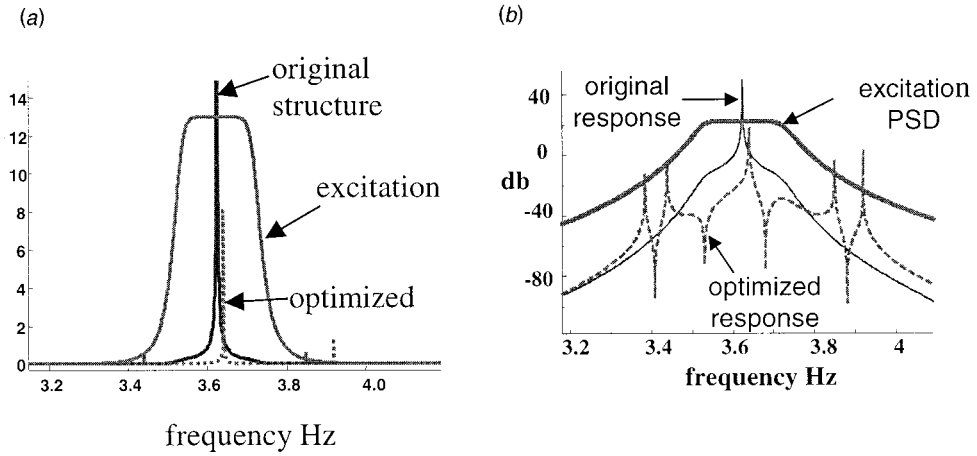

Fig. 9 Excitation PSD and the response of the initial and the optimized structures vs frequency in linear and log scales

$$\mathbf{B}=\begin{pmatrix}\binom{\mathbf{0}}{\mathbf{0}}\\ \mathbf{b_u}\\ \mathbf{b_g}\end{pmatrix} \tag{B1}$$

Sub-matrices of Eq. (*B*1) are also used and those are defined below

$$\mathbf{A_{ss}}=\begin{bmatrix}\mathbf{0} & \mathbf{I}\\ -\mathbf{M_{ss}^{-1}K_{ss}} & -\mathbf{M_{ss}^{-1}D_{ss}}\end{bmatrix} \tag{B2}$$

$$\mathbf{B_{su}}=\begin{bmatrix}\mathbf{0}\\ \mathbf{M_{ss}^{-1}C_u}\end{bmatrix},\quad \mathbf{B}_{sf}=\begin{bmatrix}\mathbf{0}\\ \mathbf{M_{ss}^{-1}C_f}\end{bmatrix} \tag{B3}$$

Appendix C—Solving a Lyapunov Equation by Means of an Eigendecomposition

A solution for the Lyapunov equation which has the form:

$$\mathbf{AR}+\mathbf{Ra^T}+\mathbf{G}=\mathbf{0} \tag{C1}$$

can be directly obtained given the eigenvalues and eigenvectors of $\mathbf{A,a^T}$ (see Skelton, 1989; Bucher and Braun, 1993), as:

$$\mathbf{R}=\mathbf{U_A Y U_a^T} \tag{C2}$$

$$\text{where}\quad \mathbf{Y}_{i,j}=-\frac{(\mathbf{U_A^{-1}GU_a})_{i,j}}{\lambda_{\mathbf{A}_i}+\lambda_{\mathbf{G}_j}} \tag{C3}$$

and spectral decomposition of **A,a** are expressed as:

$$\mathbf{A}=\mathbf{U_A}\,diag(\lambda_{\mathbf{A}})\mathbf{U}_A^{-1},\quad \mathbf{a}=\mathbf{U_a}\,diag(\lambda_{\mathbf{a}})\mathbf{U_a^{-1}}$$

The modal matrix of Eq. (*B*2) plays an important role in the solution process and following Bucher 1993, it can be expressed as

$$\mathbf{U}_{\mathbf{A}_{ss}}=\begin{bmatrix}\mathbf{\Phi_s} & \overline{\mathbf{\Phi}}_\mathbf{s}\\ \mathbf{\Phi_s\Lambda_s} & \overline{\mathbf{\Phi}}_\mathbf{s}\overline{\mathbf{\Lambda}}_\mathbf{s}\end{bmatrix} \tag{C4}$$

where $\mathbf{\Phi_s},\mathbf{\Lambda_s}$ are the eigenvectors and eigenvalues of $\mathbf{M_{ss}\Phi_s\Lambda_s^2}+\mathbf{D_{ss}\Phi_s\Lambda_s}+\mathbf{K_{ss}\Phi_s}=0$

Appendix D—Definitions of the Constraints

The constraints associated with the optimization problem as defined in Eq. (1), are computed according to the following scheme

***a*: weight limitation:** The total mass is computed directly as a volumetric integral including the parameter-dependent volume

$$\text{mass}(\theta)=\int_{V(\theta)}\rho\,d\nu\leqslant\overline{M} \tag{D1}$$

where $\overline{M}$ is the upper limit for the structural mass, ρ-mass density, $v(\theta)$-structure's volume as a function of the sought parameters

***b*: static deflection:** This constraint assures that a specified function of the static response, x_s, is bounded by our upper limit $\overline{x}$. In the example which we have provided in this work we have used:

$$\overline{x}=C(K_0^{-1}F_{static}),\quad x_s=C(K_\theta^{-1}F_{static}) \tag{D2}$$

where C is the output matrix (see Eq. (1)), K_0 is the stiffness matrix of the statically designed structure. K_θ is the parameter dependent stiffness matrix at the working point and F_{static} is the static load operating upon the structure.

***c*: geometric constraints:** $G\leqslant g(\theta)\leqslant\overline{G}$ The ability to modify the geometry may lead to nonrealizable dimensions e.g. negative thickens or dimensions that cannot be realized. For a beam whose thickness depend on the sought parameter-vector we obtain:

$$\underline{h}\leqslant h(\theta)\leqslant\overline{h} \tag{D3}$$

where $h(\theta),\underline{h},\overline{h}$ are here the working value of the beam thickness, the lower and upper bounds respectively.

References

[1] Kirsh, U., 1993, *Structural Optimization: Fundamentals and Applications*, Springer Verlag, Berlin.

[2] Haftka, R. T., 1992, *Elements of Structural Optimization*, Kluver, Dortmund.

[3] Turner, M. J., 1967, "Design of Minimum-Mass Structures With Specified Natural Frequencies," AIAA J., **5**, pp. 406–412.

[4] Taylor, J. E., 1967, "Minimum-Mass Bar for Axial Vibration at Specified Natural Frequency," AIAA J., **5**, pp. 1911–1913.

[5] Kamat, M. P., 1973, "Optimal Beam Frequencies by the FE Displacement Method," Int. J. Solids Struct. , **9**, pp. 415–429.

[6] Yamazaki, K., Sakamoto, J., and Kitano, M., 1993, "Efficient Shape Optimization Technique of a Two-Dimensional Body Based on the Boundary Element Method," Comput. Struct., **48**, No. 6, Sep. 17, pp. 1073–1081.

[7] Berebbia, C. A., 1989, *Computer Aided Optimum Design of Structures: Applications*, Springer Verlag, Berlin.

[8] Ram, Y. M., and Elhay, S., 1996, "Theory of a Multi-Degree-of-Freedom Dynamic Absorber," J. Sound Vib., **195**, No. 4, Aug 29.

[9] Asami, T., and Hosokawa, Y., 1995, "Approximate Expression for Design of Optimal Dynamic Absorbers Attached to Damped Linear Systems," Trans. Jpn. Soc. Mech. Eng., Ser. C, **61**, No. 583, Mar., pp. 915–921.

[10] Uwes, S., and Pilkey, W. D., 1996, "Optimal Design of Structures Under Impact Loading," Shock and Vibration, **3**, No. 11.

[11] Skelton, R. E., 1989, *Dynamic System Control—Linear System Analysis and Synthesis*, John Wiley and Sons, New York.

[12] Fletcher, R., 1980, "Practical Methods of Optimization," *Vol. 1, Unconstrained Optimization, and Vol. 2, Constrained Optimization*, John Wiley and Sons, New York.

[13] Bucher, I., and Braun, S. G., 1993, "Efficient Optimization Procedure for Minimizing the Vibratory Response via Redesign or Modification, Part I—Theory," J. Sound Vib., **175**, pp. 433–454.

[14] Parlett, B. N., 1998, *The Symmetric Eigenvalue Problem*, SIAM, Philadelphia.